Progress In Electromagnetics Research Letters, Vol. 34, 31–41, 2012

DUAL-WIDEBAND, MULTI-MONOPOLE-ANTENNA SYSTEM WITH A TRIANGULAR-CYLINDER SHIELDING WALL FOR WIRELESS, SURVEILLANCE-CAMERA APPLICATIONS

F.-S. Chang[1, *], W.-C. Chen[1], and S.-W. Su[2]

[1]Department of Electronics, Cheng Shiu University, Kaohsiung County, 83347, Taiwan

[2]EM & Wireless Communication R&D Div., ASUS, Taipei 11259, Taiwan

Abstract—A multi-monopole-antenna system capable of generating two wide operating bands with good input matching by a voltage standing wave ratio (VSWR) of 1.5 to cover the 2.4 GHz (2400–2484 MHz), 5.2 GHz (5150–5350 MHz), and 5.8 GHz (5725–5825 MHz) bands for wireless local area network (WLAN) applications is introduced. The design mainly comprised three, metal-plate monopole antennas symmetrically located on a main, hexagonal ground plane and backed by vertical, step-shaped grounds protruding thereon. The step-shaped grounds not only facilitated the attaining of wide impedance bandwidth but also good port isolation. In addition, directional antenna radiation was also produced. Further, a triangular-cylinder shielding wall was placed in the center of the main ground plane for integration of the wireless, surveillance-camera module into the proposed antenna system. Details of the design prototype are described and discussed in the article.

1. INTRODUCTION

Planar monopole antennas are simple in geometry and easy to construct from a simple metal plate [1–6]. This kind of antenna usually has the advantages of providing wide operating bandwidth and is achieved by mounting a metal plate on a relatively large ground plane. However, not many studies focused on grouping multiple monopoles into multi-antenna designs [7–11], which are substantially important

Received 21 May 2012, Accepted 12 July 2012, Scheduled 19 August 2012

* Corresponding author: Saou-Wen Su (susw@ms96.url.com.tw).

for multi-radio antenna system development, for signals accessing in both transmit and receive ways. Although a three-monopole antenna system was proposed for wideband operation in the 2400–5850 MHz band [7], the ground plane was still reserved for antennas only, similar to other multi-antenna designs in [8, 11]. In this Letter, we propose a new, multi-monopole-antenna system able to provide dual-wideband operation with good impedance matching (14 dB return loss) over the 2.4/5.2/5.8-GHz WLAN bands and integrating the shielding wall of the surveillance camera module into the antenna design [12]. The hollow cylinder shielding wall had a large side length and height (80 and 50 mm, respectively, in this study). A practical surveillance camera module can easily fit in the cylinder. The design consisted of a main, system ground plane and three metal-plate monopoles (size 15 mm $\times$ 21 mm) fed above small antenna grounds and backed by vertical step-shaped grounds. Each monopole was symmetrically placed with respect to the center of the main ground with equal included angles of 120° between the adjacent monopoles (see Figure 1). In this case, each antenna radiation generated equal, 3-D space coverage. The obtainable

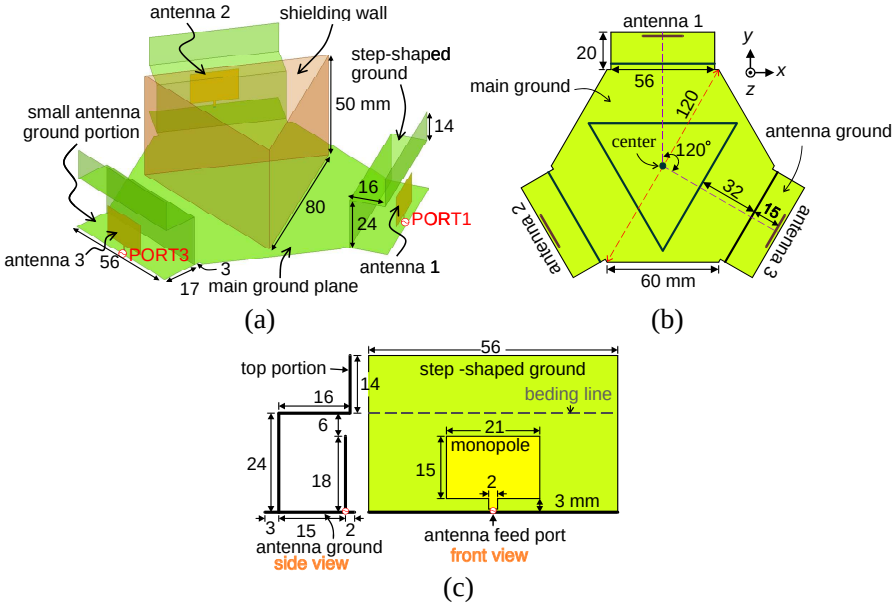

Figure 1. (a) Configuration of the proposed, dual-band, multi-monopole-antenna system for wireless, surveillance-camera applications. (b) Top view of the proposed, multi-antenna system. (c) Detailed dimensions of the metal-plate monopole (antenna 1).

impedance bandwidth and antenna port isolation were fined tuned by the parameters of the monopole and the step-shaped ground plane. A design example of the proposed antenna is demonstrated, and the experimental and simulation results are presented.

2. ANTENNA CONFIGURATION AND DESIGN CONSIDERATIONS

The methodology of the design is described here in brief. First, to attain wideband operation covering the 2.4/5.2/5.8 GHz bands, planar monopole antennas were chosen [1–6]. Second, to provide directional radiation patterns for better 3-D space coverage, vertical grounds were used. This vertical ground was also found to be beneficial to the antenna bandwidth and port isolation. Finally, a large, hollow cylinder shielding wall for accommodating some practical surveillance camera module was included. Figure 1(a) shows the configuration of a three-monopole system for 2.4-/5.2-/5.8-GHz, wireless, surveillance-camera applications. The design consisted of a main, hexagonal ground plane of side length 60 mm (the diagonal length between the two vertexes was 120 mm), three metal-plate monopoles (denoted as antennas 1, 2, 3, which were also backed by vertical, step-shaped grounds), and a triangular-cylinder shielding wall of the surveillance camera module. Each antenna was located on a small antenna ground (size 20 mm $\times$ 56 mm), which was connected to the side of the main ground plane, and next to the two no-antenna sides of the hexagonal ground with equal included angles of 120° between the adjacent monopoles. The shielding wall was placed in the center of the main ground and had a side length of about 80 mm and a height of 50 mm. In this case, the design integrated the wireless, surveillance-camera module into the multi-antenna system. Figure 1(b) presents a comprehensible, top-view drawing of the design described above. Clearly, it is seen that the three monopoles are arranged in a symmetrical fashion such that each antenna radiation covers equal 3-D space.

The near optimal dimensions of the metal-plate monopole antenna are detailed in Figure 1(c). The antenna was a rectangular planar monopole [5] with the dimensions 15 mm $\times$ 21 mm. At the center of the monopole lower edge, a feeding stub of 2 mm in width and 3 mm in length (that's feed gap) was used for easy connection, via a through-hole in the antenna ground plane, to a 50-Ω SubMiniature version A (SMA) connector for signal transmission. Notice that a 2-mm small gap between the longer edge of the antenna ground and the through-hole was reserved to accommodate the SMA connector soldered on the back side of the ground. The step-shaped ground

was formed by bending a rectangular plate two times and connected to the antenna ground at a preferred distance of 15 mm away from the monopole. This vertical ground was found to be beneficial to the obtainable impedance bandwidth and the port isolation between the antennas. The top portion of the step-shaped ground also allowed the antenna lower-edge operating frequency to be much lowered without much affecting the input matching over the attained lower operating band. A height of 14 mm for this parameter was selected. The photos of a constructed prototype are demonstrated in Figure 2. The design was fabricated from a metal plate (a 0.3-mm copper sheet was used in this study). To measure the antennas, three SMA connectors were utilized to feed the monopoles. The preferred dimensions reported in this paper were achieved by the rigorous parametric analyses with the aid of the electromagnetic-field simulation tool, Ansoft HFSS [13].

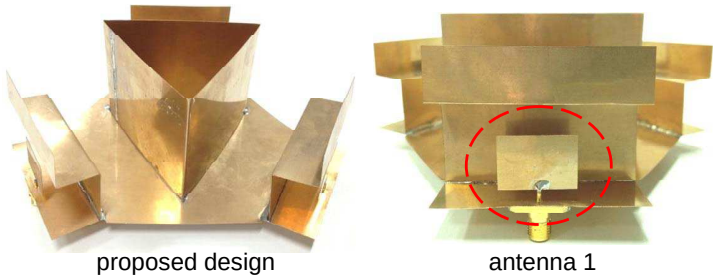

Figure 2. Photos of a constructed design prototype.

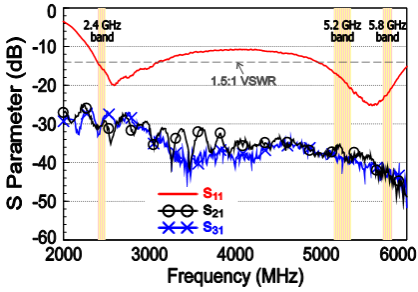

Figure 3. Measured reflection coefficient (S_{11}) and isolation (S_{21}, S_{31}) for antenna 1.

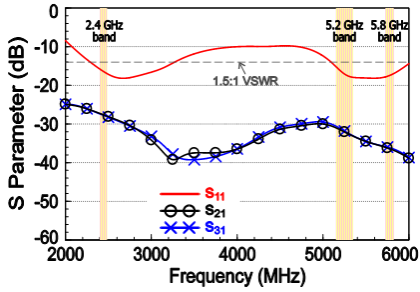

Figure 4. Simulated reflection coefficient (S_{11}) and isolation (S_{21}, S_{31}) for antenna 1.

3. RESULTS AND DISCUSSION

Prototypes of the proposed antenna as shown in Figure 2 were constructed and tested. Figure 3 shows the measured reflection coefficient (S_{11}) and isolation (S_{21}, S_{31}) between the monopoles; the simulated counterparts are given in Figure 4. The experimental data, in general, agree with the simulation results, which were based on the finite element method (FEM). Discrepancies are found due to effects of measurement cables and fabrication tolerance used in the experiments. Two wide operating bands are excited with the impedance matching over the 2.4 GHz and the 5.2/5.8 GHz bands below −14 dB (about VSWR of 1.5), which surpasses the bandwidth specification for WLAN operation in industry (usually required to be below −10 dB). For the isolation, it is found to be below −25 and −30 dB over the 2.4 and 5.2/5.8 GHz bands, respectively. As described in Section 2, this good

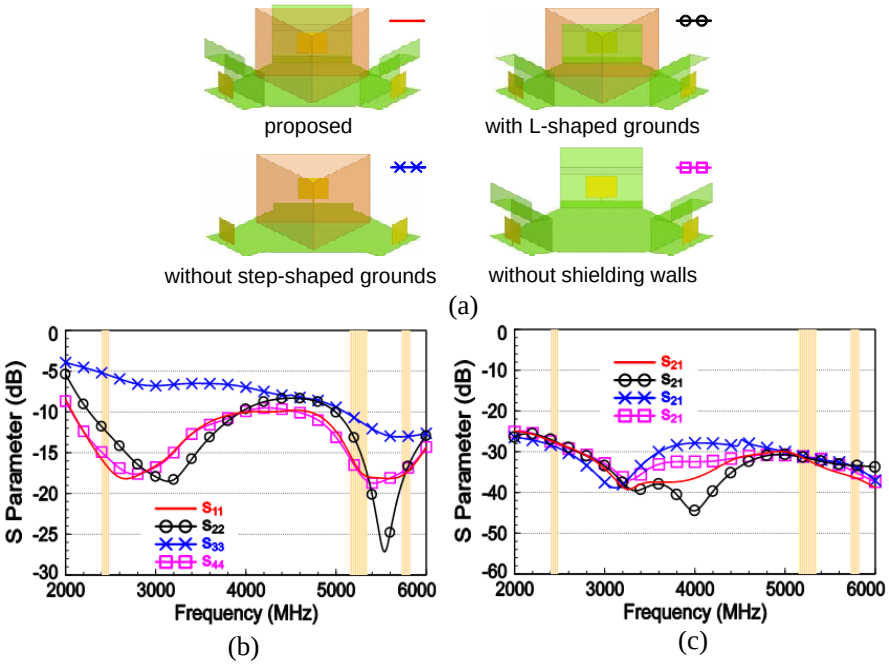

Figure 5. Simulated S-parameters for the proposed antenna (antenna 1) and the reference antennas with L-shaped grounds, without step-shaped grounds, and without central shielding wall; other dimensions remain the same as studied in Figure 4: (a) proposed and reference antennas; (b) reflection coefficients; (c) isolation between the two antennas.

decoupling resulted from the use of the vertical step-shaped grounds.

Effects of the step-shaped grounds and the central, triangular-cylinder shielding wall on the antenna operating frequencies and port isolation are studied; the results are discussed with the aid of Figure 5. Four different cases are depicted in Figure 5(a) with the antenna

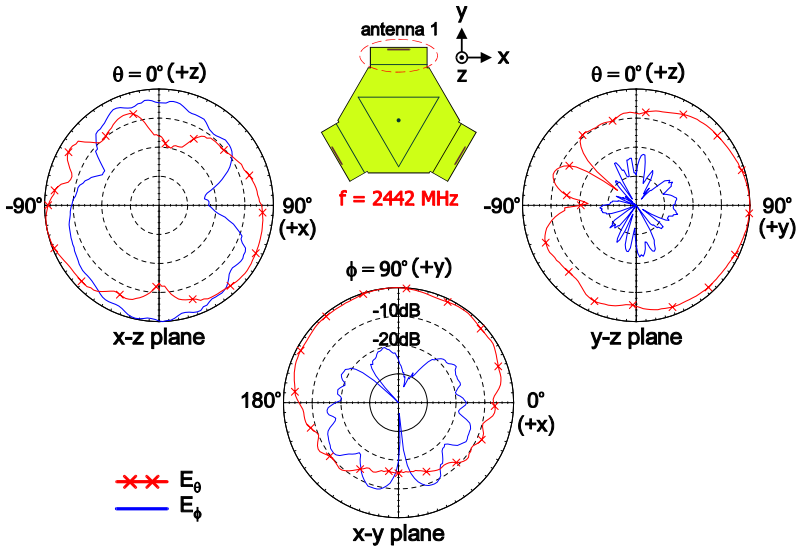

(a)

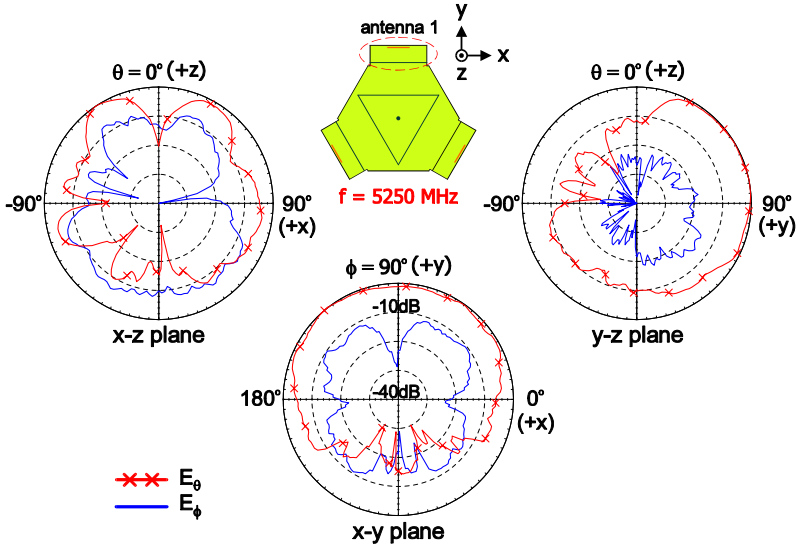

(b)

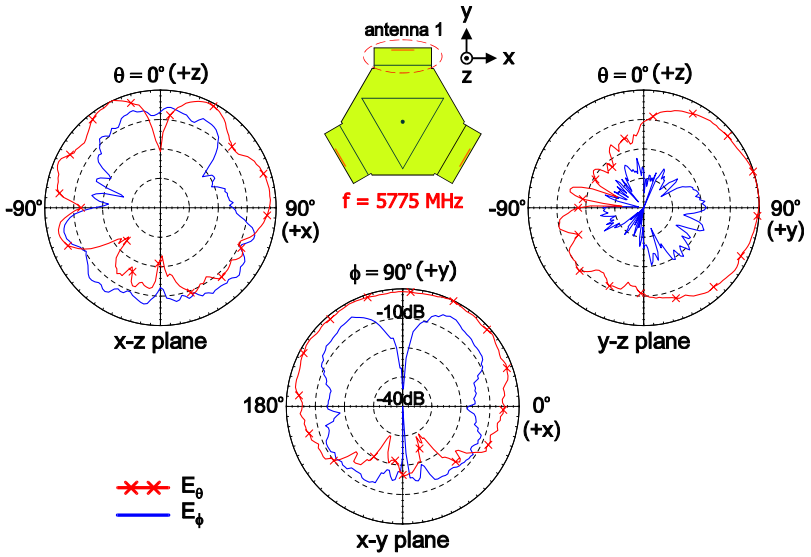

(c)

Figure 6. Measured 2-D radiation patterns at (a) 2442 MHz, (b) 5250 MHz, and (c) 5775 MHz for antenna 1 studied in Figure 3.

dimensions remaining the same as studied in Figure 4. The properties of the reflection coefficients are analyzed in Figure 5(b), while the isolation is given in Figure 5(c). First, it can be seen that without the step-shaped ground, the input matching of the antenna is devastated such that the impedance-bandwidth requirement only met a VSWR of 3 (that's, below −6 dB; see curves of S_{11} and S_{33}). Second, compared with the case of the antenna with a L-shaped ground (that's, to remove the top portion of the step-shaped ground; see curve S_{22}), the lower-edge operating frequency for the proposed antenna is much lower by 295 MHz (from 2585 to 2290 MHz defined by VSWR of 1.5). This suggests that the monopole antenna could even be smaller in size. Finally, the reflection-coefficient parameters are similar between the case of no central shielding wall (see curve S_{44}) and the proposed antenna. This phenomenon is straightforward because the step-shaped ground also shields the partial radiation of the monopole toward to the center. In this case, the conducting elements put behind the step-shaped ground have fewer effects on the antenna impedance bandwidth. As for the isolation characteristics, the results show that the variation within the bands of interest is quite small.

The over-the-air (OTA) performance of the prototype was studied. Figures 6 and 7 show the measured and simulated, 2-D radiation patterns in E_θ and E_φ fields. Notice that the radiation patterns are

normalized with respect to the peak antenna gain in each pattern cut. For brevity the patterns are only presented at 2442, 5250, and 5775 MHz, the central frequencies of the three WLAN bands. In addition, due to the three identical antennas symmetrical in

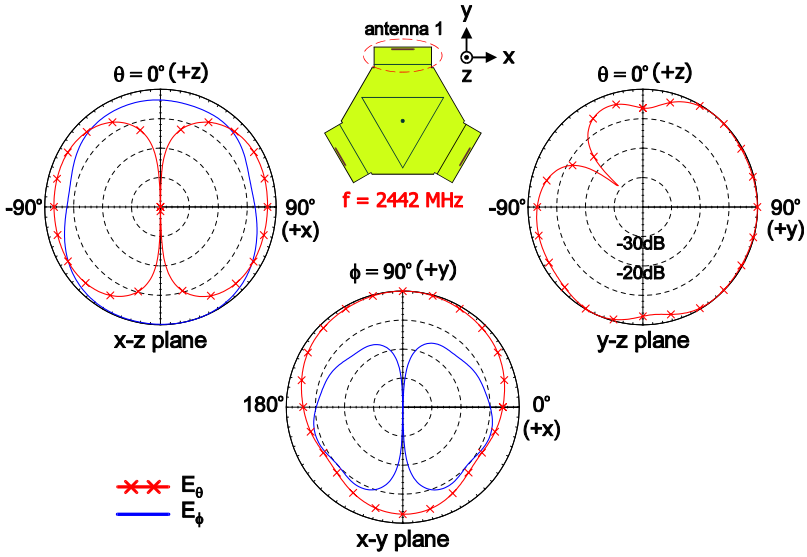

(a)

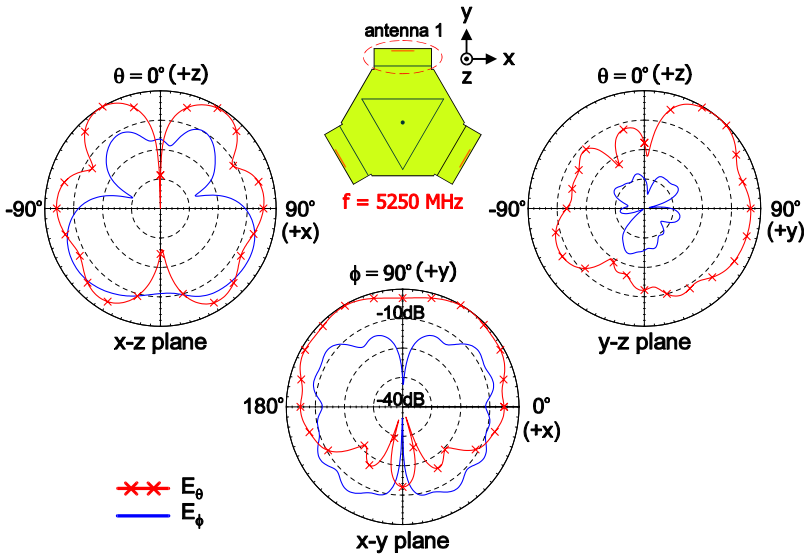

(b)

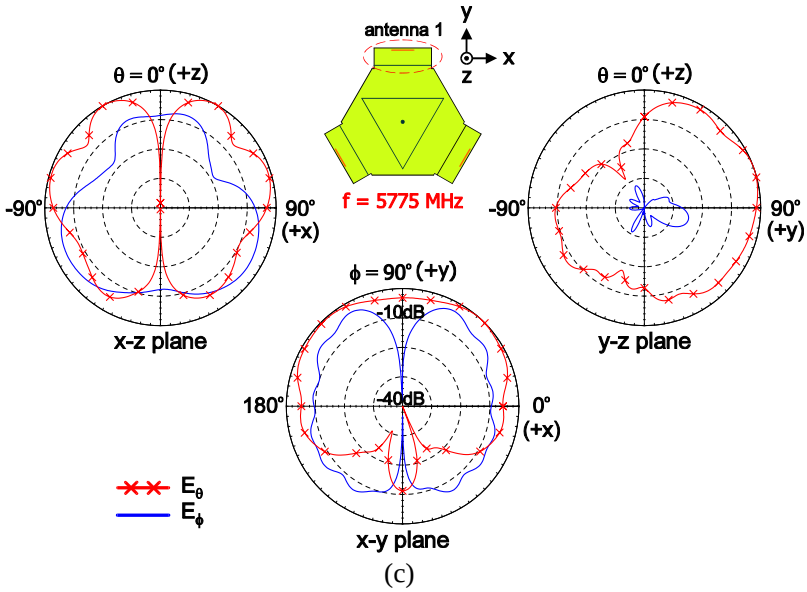

(c)

Figure 7. Simulated 2-D radiation patterns at (a) 2442 MHz, (b) 5250 MHz, and (c) 5775 MHz for antenna 1 studied in Figure 4.

arrangement, only radiation patterns of antenna 1 are shown. Overall, the measured results compare favorably to the simulation. The directional patterns are first observed in the x-y and y-z planes. This directional radiation characteristic is also found for the antenna excited at other frequencies across the operating bandwidth. Second, E_θ fields (that's, copolarization in this study) are relatively large compared with E_φ fields in the y-z planes. On the other hand, comparable E_θ and E_φ fields are observed in the x-z planes. This is because that the antenna copolarization is mainly contributed from the excited surface currents in the radiating monopole element. Conversely, the cross-polarization is contributed from the image currents in the main ground plane and step-shaped ground, which are symmetrical with respect to the y-z plane. The cross-polarization can be thus canceled out, leading to less E_φ fields in the y-z plane.

Figure 8 plots the measured, peak antenna gain and the radiation efficiency against frequency for the proposed antenna. The peak gain over the 2.4 GHz band is as seen at a constant level of about 2.9 dBi with the radiation efficiency exceeding 75%, which corresponds to the total radiated power (TRP) of -2.87 dBm when the given antenna input power is 0 dBm. For the upper bands, including the 5.2 and 5.8 GHz bands, the peak gain is in the range of 4.6 to 5.8 dBi with the radiation efficiency larger than 70%, corresponding to the TRP

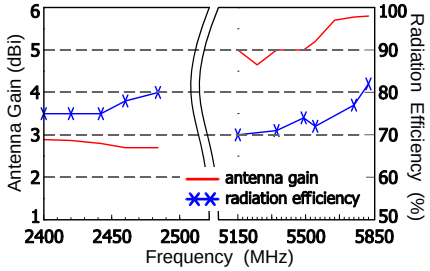

Figure 8. Measured, peak antenna gain and radiation efficiency against frequency for antenna 1 studied in Figure 6.

of −3.56 dBm. Notice that the radiation efficiency was obtained by calculating the TRP of the antenna under test (AUT) over the 3-D spherical radiation first and then dividing that total amount by the input power of 0 dBm given to the AUT. The gain measurement also took account of the mismatch of the antenna input impedance, and the "realized gain" [14] was measured.

4. CONCLUSION

A dual-wideband, three-antenna system utilizing planar, wideband monopole antennas, backed by step-shaped grounds, and integrating the shielding wall of the surveillance camera module into the antenna design for 2.4- and 5.2/5.8-GHz WLAN operation has been demonstrated, studied, and tested. The impedance matching for the obtainable bandwidth within the bands of interest is less than −14 dB. The isolation between any two monopoles is well below −25 dB across the desired operating frequencies and even less than −30 dB in the upper operating bands. The low mutual coupling is due largely to the incorporation of the step-shaped grounds. Directional radiation patterns with the peak antenna gain of about 2.9 and 5.8 dBi for the 2.4 and 5 GHz monopoles has been obtained, too. The proposed antenna is well suited for wireless, surveillance-camera applications.

REFERENCES

1. Agrawall, N. P., G. Kumar, and K. P. Ray, "Wide-band planar monopole antennas," *IEEE Trans. Antennas Propagat.*, Vol. 46, 294–295, 1998.
2. Ammann, M. J., "Square planar monopole antenna," *Proc. IEE National Conf. Antennas Propagat.*, 37–40, UK, 1999.

3. Ammann, M. J. and Z. N. Chen, "Wideband monopole antennas for multi-band wireless systems," *IEEE Trans. Antennas Propagat. Mag.*, Vol. 45, 146–150, 2003.
4. Su, S. W., K. L. Wong, and C. L. Tang, "Ultra-wideband square planar monopole antenna for IEEE 802.16a operation in the 2–11 GHz band," *Microwave Opt. Technol. Lett.*, Vol. 42, 463–466, 2004.
5. Su, S. W., K. L. Wong, Y. T. Cheng, and W. S. Chen, "Finite-ground-plane effects on the ultra-wideband planar monopole antenna," *Microwave Opt. Technol. Lett.*, Vol. 43, 535–537, 2004.
6. Wong, K. L., C. H. Wu, and S. W. Su, "Ultra-wideband square planar metal-plate monopole antenna with a trident-shaped feeding strip," *IEEE Trans. Antennas Propagat.*, Vol. 53, 1262–1269, 2005.
7. Chou, J. H. and S. W. Su, "Internal wideband monopole antenna for MIMO access-point applications in the WLAN/WiMAX bands," *Microwave Opt. Technol. Lett.*, Vol. 50, 1146–1148, 2008.
8. Su, S. W., "High-gain dual-loop antennas for MIMO access points in the 2.4/5.2/5.8 GHz bands," *IEEE Trans. Antennas Propagat.*, Vol. 58, 2412–2419, 2010.
9. Su, S. W. and T. C. Hong, "Printed, multi-loop-antenna system integrated into a concurrent, dual-WLAN-band access point," *Microwave Opt. Technol. Lett.*, Vol. 53, 317–322, 2011.
10. Su, S. W. and C. T. Lee, "Low-cost dual-loop-antenna system for dual-WLAN-band access points," *IEEE Trans. Antennas Propagat.*, Vol. 59, 1652–1659, 2011.
11. Su, S. W., "Integration of loop and slot antennas into one-piece metal plate for concurrent 2.4- and 5-GHz wireless local area network operation," *Microwave Opt. Technol. Lett.*, Vol. 54, 815–820, 2012.
12. Chien, S. L., F. R. Hsiao, Y. C. Lin, and K. L. Wong, "Planar inverted-F antenna with a hollow shorting cylinder for mobile phone with an embedded camera," *Microwave Opt. Technol. Lett.*, Vol. 41, 418–419, 2012.
13. Ansoft Corporation HFSS, Pittsburgh, PA, http://www.ansoft.com/products/hf/hfss.
14. Volakis, J. L., *Antenna Engineering Handbook,* 4th Edition, Chapter 6, 16–19, McGraw-Hill, New York, 2007.